# Smooth band termination in $^{108}$Sn

R. Wadsworth,[1] C. W. Beausang,[2] M. Cromaz,[3] J. DeGraaf,[3] T. E. Drake,[3] D. B. Fossan,[4] S. Flibotte,[5] A. Galindo-Uribarri,[6] K. Hauschild,[1] I. M. Hibbert,[1] G. Hackman,[5] J. R. Hughes,[4,*] V. P. Janzen,[6] D. R. LaFosse,[4,†] S. M. Mullins,[5,‡] E. S. Paul,[2] D. C. Radford,[6] H. Schnare,[4,§] P. Vaska,[4] D. Ward,[6] J. N. Wilson,[5] and I. Ragnarsson[7]

[1]*Department of Physics, University of York, Heslington, York Y01 5DD, United Kingdom*

[2]*Oliver Lodge Laboratory, University of Liverpool, Liverpool L69 3BX, United Kingdom*

[3]*Department of Physics, University of Toronto, Toronto, Ontario, Canada M5S 1A7*

[4]*Department of Physics, S.U.N.Y. at Stony Brook, Stony Brook, New York 11794*

[5]*Department of Physics and Astronomy, McMaster University, Hamilton, Ontario, Canada L8S 4M1*

[6]*Chalk River Laboratories, AECL, Chalk River, Ontario, Canada K0J 1J0*

[7] *Department of Mathematical Physics, Lund Institute of Technology, P.O. Box 118, S-221 00, Lund, Sweden*

(Received 10 October 1995)

Three rotational bands in $^{108}$Sn have been investigated to high frequency via the $^{54}$Fe($^{58}$Ni,4$p$) reaction at 243 MeV. One of these bands is observed to undergo a band crossing at high spin. All three bands show a large decrease in their dynamic moments of inertia, to approximately one third of the rigid body value, as the rotational frequency approaches 1 MeV/$\hbar$. The structures of these bands are thought to be based on 2p-2h proton excitations across the $Z=50$ shell gap and their properties can be interpreted in terms of cranked Nilsson-Strutinsky calculations. Such calculations predict smooth band terminations for all three structures and a gradual shape change from collective prolate, at low spin, to noncollective oblate at high spin. [S0556-2813(96)00105-7]

PACS number(s): 21.10.Re, 27.60+j, 23.20.Lv

## I. INTRODUCTION

Previous work on $^{108}$Sn has identified three rotational bands [1] which dominate the high spin structure. One of these bands was assigned positive parity whilst the remaining two bands were tentatively assigned as having negative parity. The properties of these bands are very similar to those of rotational bands observed in odd-$A$ Sb nuclei (e.g., [2,3]), which have recently been interpreted as resulting from a smooth transition from a prolate collective shape at low rotational frequencies, to a noncollective oblate shape at the highest frequencies observed. This situation has been shown to arise when a particular valence configuration evolves continuously from high collectivity at low spin to a point where all the spin vectors of the particles involved in the configuration are maximally aligned, and has been called a ''smooth'' or ''soft'' terminating band [4]. This feature is very different to the other cases where ''abrupt'' or ''sudden'' band termination has been observed (e.g., $^{158}$Er [5], $^{122}$Xe [6]). Here terminating states of maximal spin have been identified but their valence configurations are not the same as those of the collective bands which dominate the spectroscopy at lower spins. In this case the oblate noncollective states cross the prolate collective states and become yrast at high spin.

The bands in $^{108}$Sn have previously been interpreted as being built on $\pi(g_{9/2}^{-2}\otimes g_{7/2}^{2})$ and $\pi(g_{9/2}^{-2}\otimes g_{7/2}^{1}h_{11/2}^{1})$ 2p-2h proton excitations across the $Z=50$ shell gap, with aligned $h_{1/2}$ neutrons also being involved in the configurations [1]. Related 2p-2h structures were first discovered in the heavier even-$A$ tin isotopes by Bron *et al.* [7]. In the earlier work on $^{108}$Sn [1] only one of the three bands had been linked into the known level scheme [8], thus making the assignment of the configurations somewhat tentative. Also, in that work it was not possible to confirm the spin assignments given by Azaiez *et al.* [8] for the positive parity band (band 1 of [1]) since there were insufficient statistics to allow a directional correlation analysis (DCO) to be performed for the weak high-energy linking transitions below the band.

In order to further investigate the above problems we have obtained new data on the rotational bands in $^{108}$Sn. In the present work we report the observation of linking transitions for one of the two previously unconnected bands and also the measurement of DCO ratios for linking transitions from the two bands which are now connected. These results have enabled us to obtain new spin assignments for both of these bands. There is also evidence for a band crossing in the positive parity band at high spin. This feature is discussed within the Nilsson-Strutinski cranking model. Finally, the structures of all the bands are compared with calculations based on this model.

## II. EXPERIMENTAL DETAILS AND DATA ANALYSIS

Data from two different experiments have been used in this work. In both cases, the levels in $^{108}$Sn were populated via the $^{54}$Fe($^{58}$Ni,4$p$) reaction at a beam energy of 243 MeV.

*Current address: Lawrence Livermore Laboratory, P.O. Box 808, Livermore, CA 94550.

†Current address: Chemistry Department, Washington University, St. Louis, MO 63130.

‡Current address: Department of Nuclear Physics, RSPhysSE, The Australian National University, Canberra ACT 0200, Australia.

§Current address: Research Centre Rossendorf, PF 510119, D-01314 Dresden, Germany.

 

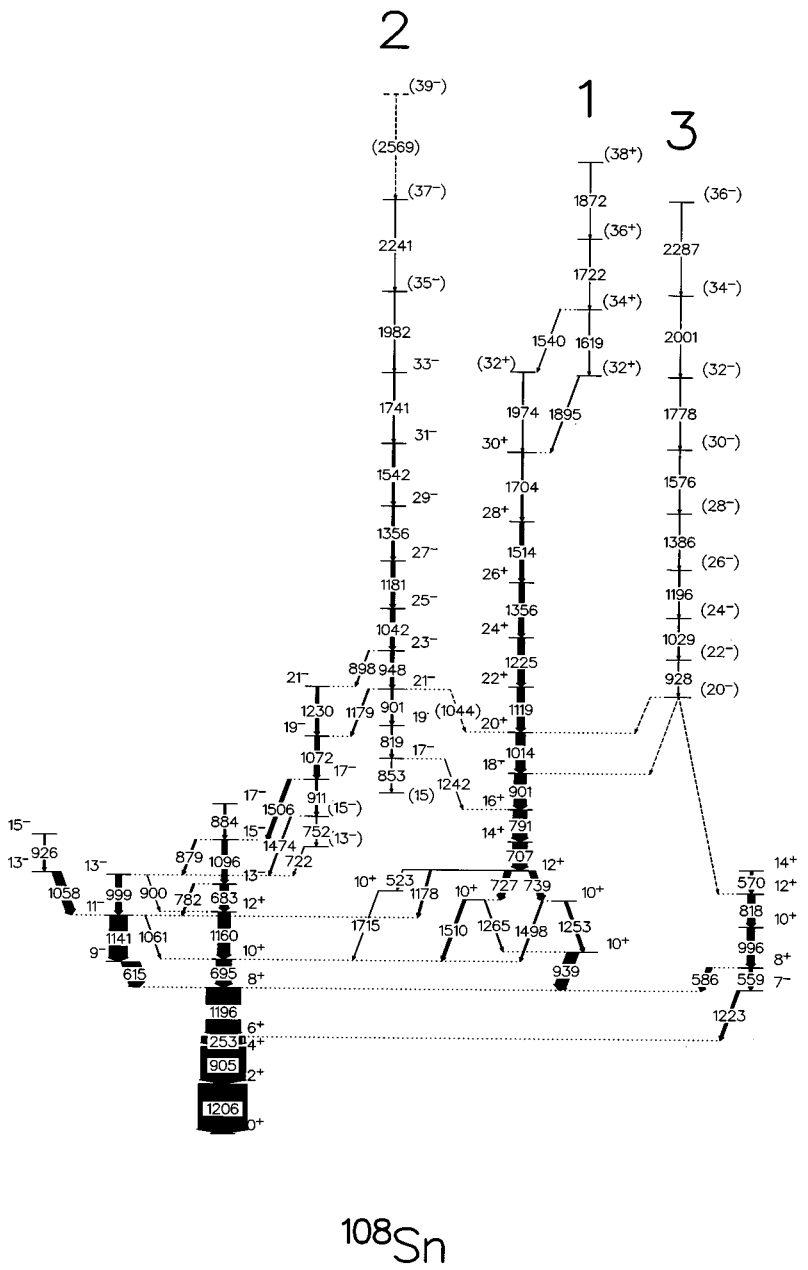


FIG. 1. Partial decay scheme for $^{108}$Sn deduced from this work. Gamma-ray intensities are proportional to the widths of the arrows. The dashed transitions from the bottom of band 3 do not necessarily represent single unobserved gamma rays.

The energy was chosen to be the same as in previous studies [1].

The high spin properties of $^{108}$Sn were investigated with the early implementation of the Gammasphere $\gamma$-ray detector array. At that time, the array consisted of 24 bismuth-germanate (BGO)-suppressed HPGe detectors, each with an efficiency of approximately 75% relative to a $3\times3$ sodium iodide crystal at 1.3 MeV. In this particular experiment the target consisted of two stacked 0.5 mg/cm$^2$ foils of $^{54}$Fe with an enrichment of 97%. The multifold event by event data were analyzed as follows. First, the events were unpacked into threefold coincidences and used to produce an $E_\gamma$-$E_\gamma$-$E_\gamma$ cube which contained $3.9\times10^8$ triples events. The triples data were also used to produce $E_\gamma$-$E_\gamma$ matrices. In this case the third gamma ray was used as a gate. This produced ''clean'' matrices for studying the various rotational bands. Information from these matrices and the cube was used in order to determine the transitions at the top of the three known rotational bands. Analysis was carried out using the graphical analysis programs LEVIT8R (cube) and ESCL8R (matrices) [9]. These programs enabled the level scheme to be deduced from the coincidence relationships and relative intensities of the gamma rays. In this early implementation of Gammasphere there were no detectors close to 90° to the beam direction, and consequently, it was not possible to perform a directional correlation analysis.

In the second experiment, gamma rays were detected using the Chalk River $8\pi$ spectrometer array. For a valid coincidence event 9 or more of the BGO inner ball crystals ($K\geqslant9$) were required in addition to two Compton suppressed HPGe counters; a total of $7\times10^8$ such events were acquired. The target consisted of 580 $\mu$g/cm$^2$ $^{54}$Fe, enriched to $>95\%$, on a 25 mg/cm$^2$ thick gold backing. In order to enhance the four-particle reaction channel the data were sorted off line, with a filter on the BGO ball requiring $8\leqslant K\leqslant16$, into an angular-correlation matrix which contained

data from detectors at $\theta = \pm 79°$ with respect to the beam direction along one axis and data from detectors at $\theta = \pm 37°$ along the other axis. Coincident $\gamma$-ray intensity ratios $[I_\gamma(37°-79°)/I_\gamma(79°-37°)]$, obtained from this matrix, were used to determine stretched-dipole, stretched-quadrupole, and unstretched-quadrupole transitions using the method of directional correlation from oriented (DCO) states [10]. In this geometry, intensity ratios of 1.0 are predicted for a stretched-quadrupole–stretched-quadrupole correlation and $\sim 0.6$ for a stretched-quadrupole–stretched-dipole correlation with no mixing [11]. Values greater than or less than 1.0 are possible for mixed $M1/E2$ transitions (i.e., $J \rightarrow J \rightarrow J-2$ correlation) depending on the sign of the multipole mixing ratio. In the present work, only strong stretched $E2$ quadrupole transitions were used as gating transitions.

These backed-target data were used to obtain DCO ratios for transitions below the rotational structures in $^{108}$Sn. These decays are emitted after the recoiling nuclei have stopped in the gold backing. The data could not, however, be used to obtain DCO ratios for transitions within the rotational bands (with the exception of the lowest two transitions in band 1) as the collectivity of these structures results in Doppler smearing as the gamma rays are emitted while the nuclei are slowing down in the target and gold backing.

## III. EXPERIMENTAL RESULTS

Previous work on $^{108}$Sn [1] has identified three rotational bands which dominate at high spin. The present work has enabled us to study the highest spins in these bands and to link in one of the two previously unconnected bands to the spherical levels at low spin. We have also been able to measure DCO ratios which has enabled us to determine the spins of the two bands which are now linked into the main decay scheme.

The decay scheme deduced for $^{108}$Sn from the present work is shown in Fig. 1. Figure 2 shows the double-gated gamma-ray spectra obtained from the thin-target cube for the three previously reported intruder bands. The spectra are the sums of double-gate combinations of all the gamma rays in each of the bands shown.

Band 1 had previously been observed up to the 1895 keV transition. The present work has extended this and shows that there is in fact a band crossing occurring beyond spin 30 $\hbar$. The spins of the levels in this band are different to those given in [1,8]. Those presented in [1] were in fact taken from [8] as it was not possible to measure DCO ratios for the high-energy transitions below this band in the former experiment. In the present work we have been able to determine new DCO ratios for these transitions. Results for the transitions of interest are presented in Table I. The DCO ratios for the 523, 727, 739, and 939 keV transitions, which depopulate band 1, clearly support pure $E2$ assignments for these gamma rays. The intermediate levels which are populated by the decay of the 727 and 739 keV transitions decay via high energy gamma rays which have DCO ratios of approximately 0.8. This is indicative of mixed $M1/E2$ transitions with no parity change and a spin change of either one or zero. However, only the latter option, which leads to a spin-parity assignment of $12^+$ for the lowest level of band 1, is consistent with the DCO ratio for the 1178 keV transition

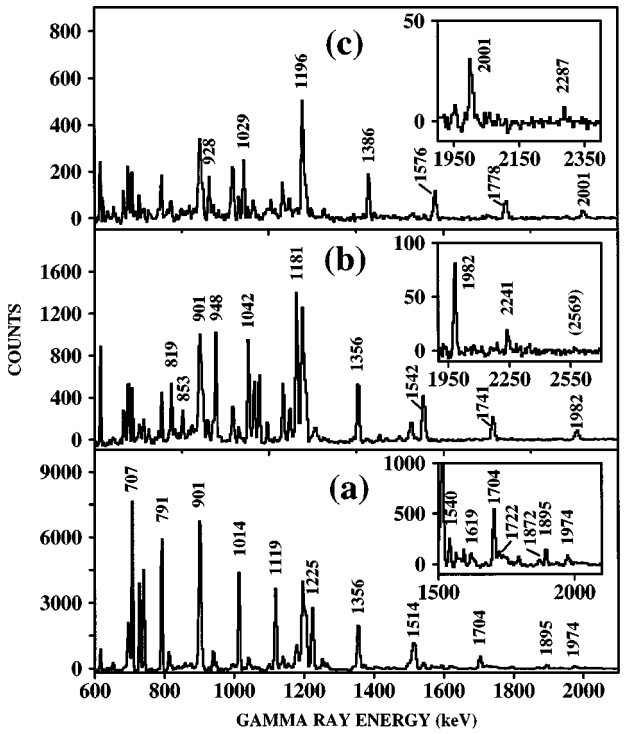


FIG. 2. Spectra showing the three rotational bands in $^{108}$Sn (a) band 1, (b) band 2, and (c) band 3. Transitions within each of the bands are labeled. These spectra are the results of all possible combinations of double gates on the members of each band from a RADWARE cube.

which depopulates that level. Thus the present results indicate that the lowest level of band 1 has a spin and parity of $12^+$, not $14^+$ as previously published. It was not possible to obtain DCO ratios for any of the new transitions at the top of this band as the intensities fall off rapidly (e.g., the uppermost 1872 keV transition is estimated to be $\sim 3\%$ of that of the 707 keV $\gamma$ ray). Consequently, we have assumed that the 1619, 1895, 1974, 1540, 1722, and 1872 keV gamma rays are stretched $E2$ transitions.

TABLE I. Angular correlation ratios for transitions below band 1 in $^{108}$Sn. One $E2$ transition from the bottom of band 1 (707 keV) is included for comparison. ($*$) Too weak to measure.

| $E_\gamma$ (keV) | $\frac{I(37-79)}{I(79-37)}$ | Assignment $J_i^\pi \rightarrow J_f^\pi$ |
|---|---|---|
| 523 | 1.09(10) | $12^+ \rightarrow 10^+$ |
| 707 | 1.02(2) | $14^+ \rightarrow 12^+$ |
| 727 | 1.00(6) | $12^+ \rightarrow 10^+$ |
| 739 | 1.10(7) | $12^+ \rightarrow 10^+$ |
| 939 | 1.01(5) | $10^+ \rightarrow 8^+$ |
| 1178 | 0.62(6) | $12^+ \rightarrow 11^-$ |
| 1253 | 0.85(5) | $10^+ \rightarrow 10^+$ |
| 1265 | 0.83(5) | $10^+ \rightarrow 10^+$ |
| 1498 | 0.78(8) | $10^+ \rightarrow 10^+$ |
| 1510 | 0.79(4) | $10^+ \rightarrow 10^+$ |
| 1715 | $*$ | $10^+ \rightarrow 10^+$ |

TABLE II. Angular correlation ratios for transitions from negative-parity levels above the yrast $12^+$ level in $^{108}$Sn.

| $E_\gamma$ (keV) | $\frac{I(37-79)}{I(79-37)}$ | Assignment $J_i^\pi \rightarrow J_f^\pi$ |
|---|---|---|
| 683 | 0.55(6) | $13^- \rightarrow 12^+$ |
| 722 | 0.77(12) | $(13^-) \rightarrow 13^-$ |
| 752 | 0.94(20) | $15^- \rightarrow (13^-)$ |
| 884 | 0.97(9) | $17^- \rightarrow 15^-$ |
| 898 | 0.97(10) | $23^- \rightarrow 21^-$ |
| 911 | 1.02(7) | $17^- \rightarrow 15^-$ |
| 1072 | 0.97(9) | $19^- \rightarrow 17^-$ |
| 1096 | 1.00(7) | $15^- \rightarrow 13^-$ |
| 1179 | 0.97(11) | $21^- \rightarrow 19^-$ |
| 1230 | 1.00(11) | $21^- \rightarrow 19^-$ |
| 1474 | 1.10(12) | $15^- \rightarrow 13^-$ |
| 1506 | 0.98(8) | $17^- \rightarrow 15^-$ |

The improved quality and quantity of the data from the third-generation Gammasphere array has enabled us to link band 2 to the low lying levels. In the present work approximately 50% of the decay-out intensity of this band has been observed. This is the sum of intensities of the 898, 1179, and 1242 keV $\gamma$ rays, which contribute $\sim$10%, $\sim$40%, and $<$5%, respectively. DCO ratios for the relevant transitions above the 1160 keV $12^+ \rightarrow 10^+$ transition are given in Table II. These support the spin assignments given in Fig. 1 for band 2. The DCO ratios for all other transitions which are not listed are consistent with the multipolarity assignments given in Refs. [1,8]. Previous work [1] placed the 948 keV transition directly above the 819 keV gamma ray. The triples data have enabled us to show, however, that there is in fact a 901 keV transition between these two gamma rays. Furthermore, in [1] it was tentatively suggested that there was a 2540 keV gamma ray on top of the 2241 keV transition. This could not be observed in the present work; however, we do have tentative evidence for a 2569 keV gamma ray [see Fig. 2(b)].

Band 3 still remains unconnected to the main part of the level scheme. This is the weakest of the three bands; the lower members having approximately 2% of the intensity of the $6^+ \rightarrow 4^+$ yrast transition (bands 1 and 2 have $\sim$8% and 30%, respectively). Transitions within the band are assumed to have $E2$ multipolarities. The present work has enabled us to extend this band by one transition (928 keV) below the 1029 keV gamma ray. At the top of the band the previous work [1] suggested a tentative 2277 keV transition; this could not be confirmed. There is however evidence for a weak transition of 2287 keV above the 2001 keV gamma ray in this band [see Fig. 2(c)]. The triples data still support the decay of this band into band 1 above the 1014 keV gamma ray, however the intensity of the branch is too weak to enable us to assign a specific pathway. There is also very weak evidence that some higher members of the band see the 1119 keV transition in band 1 (not shown in Fig. 1). Band 3 possesses a weak decay branch to the positive parity structure shown on the right-hand side of Fig. 1.

The tentative spins and parities of band 3, shown in Fig. 1, have been assigned on the basis of a comparison with calculations presented in the discussion section and also on where the band is experimentally observed to feed into band 1.

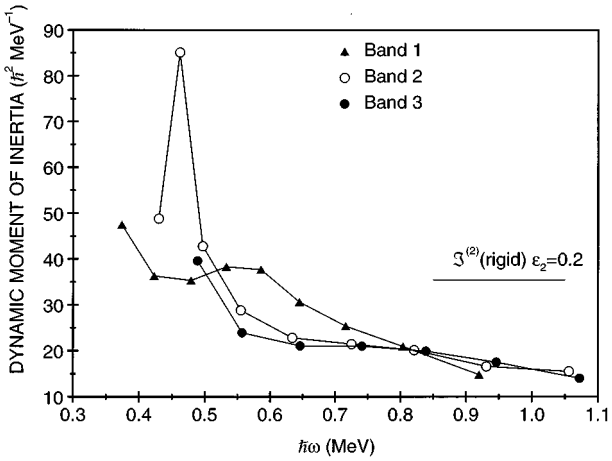


FIG. 3. Dynamic moments of inertia versus rotational frequency for the three rotational bands in $^{108}$Sn. Also shown is the moment of inertia for a rigid body with a quadrupole deformation $\epsilon_2 = 0.2$.

## IV. DISCUSSION

The low spin structure of $^{108}$Sn is dominated by spherical states in which the valence neutrons occupy the low lying $\nu g_{7/2}, \nu d_{5/2}$, and $\nu h_{11/2}$ orbitals. A discussion of the structure of the low-spin states is presented in [8] and will not be repeated here. The main focus of this paper is the high spin states, which are dominated by rotational type structures. In previous work [1] these have been discussed in terms of proton $\pi(g_{9/2}^{-2} \otimes g_{7/2}^{2})$ and $\pi(g_{9/2}^{-2} \otimes g_{7/2}^{1} h_{11/2}^{1})$ 2p-2h excitations across the $Z=50$ closed shell. The present work focuses on their interpretation in terms of the smooth band termination calculations of Ragnarsson *et al.* [4] (see also Afanasjev and Ragnarsson [12]). These calculations will be discussed in Sec. IV B below.

### A. Dynamic moments of inertia

Figure 3 shows the dynamic ($\mathcal{J}^{(2)}$) moments of inertia for the three bands observed in the present work. Previous work indicated that all three structures probably involved an aligned pair of $h_{11/2}$ neutrons. Indeed, cranking calculations showed that these were expected to align at a low rotational frequency of around 0.35 MeV/$\hbar$ for a quadrupole deformation consistent with that measured for band 1 (i.e., $\epsilon_2 = 0.2$) [1]. Furthermore the higher frequency hump around $\hbar\omega \sim 0.55$ MeV in band 1 was attributed to the alignment of the proton $g_{7/2}$ pair of particles. The absence of such an alignment in bands 2 and 3 can be taken as evidence of a different proton configuration for these structures; that is $\pi(g_{9/2}^{-2} \otimes g_{7/2}^{1} h_{11/2}^{1})$ as suggested previously. The new data from the present work show that bands 2 and 3 now exhibit very similar behavior for their dynamic moments of inertia (see Fig. 3). This supports the previous suggestion that the two bands are signature partners.

Figure 3 also shows that the $\mathcal{J}^{(2)}$ moments of inertia of all three bands gradually reduce to approximately one-third of the rigid-body value (assuming $\epsilon_2=0.2$) at very high rotational frequencies. This feature is characteristic of smoothly terminating bands and has been seen in several other nuclei (e.g., [13–15]) and reproduced in theoretical calculations [4,13]. Such behavior suggests that the individual particle spin contributions (from particles involved in the valence configuration) to the total spin of a state is significant at high rotational frequency. This naturally leads to a reduction in collectivity for the structures.

### B. Smooth band termination calculations

Calculations have been performed for $^{108}$Sn in order to investigate the high spin features and underlying configurations of the three rotational bands. The calculations were carried out with the Nilsson-Strutinsky method [16] and employed a modified oscillator potential. They also utilized new techniques [4] for identifying the $N=4g_{9/2}$ holes and $g_{7/2}$, $d_{5/2}$ particles. In the model, the energy is minimized with respect to the deformation parameters $\epsilon_2$, $\epsilon_4$, and $\gamma$.

Figure 4(b) shows the lowest-energy calculated configurations in the spin range of interest. These are 2p-2h configurations and their structures are given in the figure. Figure 4(a) shows the equivalent experimental data for the three bands in $^{108}$Sn. The experimental excitation energy of band 3 was chosen to be consistent with that for its assumed signature partner, band 2.

Clearly there is remarkable agreement between the calculated and experimental data. The calculations predict that the positive parity $\pi[g_{9/2}^{-2}\otimes(g_{7/2}d_{5/2})^2]\otimes\nu[(d_{5/2}g_{7/2})^6h_{11/2}^2]$ configuration should be crossed by the $\pi[g_{9/2}^{-2}\otimes(g_{7/2}^1h_{11/2}^1)]\otimes\nu[(d_{5/2}g_{7/2})^5h_{11/2}^3]$ positive parity configuration at spin $32\hbar$. This is precisely where band 1 is observed to undergo a band crossing. We therefore assign the upper and lower parts of this band to these two configurations, respectively. It is also interesting to note that the configuration change is the same for both protons and neutrons. Unfortunately, however, neither structure is observed to its terminating spin.

A further point of interest is the interaction strength between the yrast and yrare $32^+$ states. The decay of the $34^+$ state to the two $32^+$ states proceeds via the 1540 and 1619 keV $\gamma$ rays, which carry $\sim$60% and $\sim$40%, respectively, of the total decay intensity. If the assumption is made that there is no mixing between the observed $34^+$ state and that resulting from a continuation of the $\pi[g_{9/2}^{-2}\otimes(g_{7/2}d_{5/2})^2]\otimes\nu[(d_{5/2}g_{7/2})^6h_{11/2}^2]$ configuration (the latter would be expected to lie $\sim$600 keV higher in excitation from theoretical calculations), then an interaction strength of the order of 40 keV is obtained between the two bands. This is somewhat larger than might be expected given the differences between the two configurations. It is interesting to note, however, that the orbitals which are involved in the configuration differences ($d_{5/2}$, $g_{7/2}$, and $h_{11/2}$ for both protons and neutrons) are the same as those which lead to sizable octupole correlations in the neighboring isotone $^{110}$Te [17].

Band 2 is well explained as the favored signature of the lowest negative parity $\pi[g_{9/2}^{-2}\otimes(g_{7/2}^1h_{11/2}^1)]\otimes\nu[(d_{5/2}g_{7/2})^6h_{11/2}^2]$ configuration. The same configuration (not specifying the $d_{5/2}$, $g_{7/2}$ neutrons) was originally suggested for this structure in [1], based on the fact that the proton $g_{7/2}$ alignment was not observed. The terminating spin for the favored signature of this structure is $39^-$. The experimental data show that, with this configuration assignment, band 2 is seen to the penultimate transition ($37^-$). There is however tentative evidence for a 2569 keV transition from the final terminating state [see Fig. 2(b)]. It is worth noting that in $^{109}$Sb, where all three bands were tentatively observed to their respective terminating states, the final transition in each band was very much weaker, and hence much more difficult to identify than the penultimate transition [13]. It is perhaps not surprising, therefore, that the terminating state in $^{108}$Sn band 2 is difficult to observe.

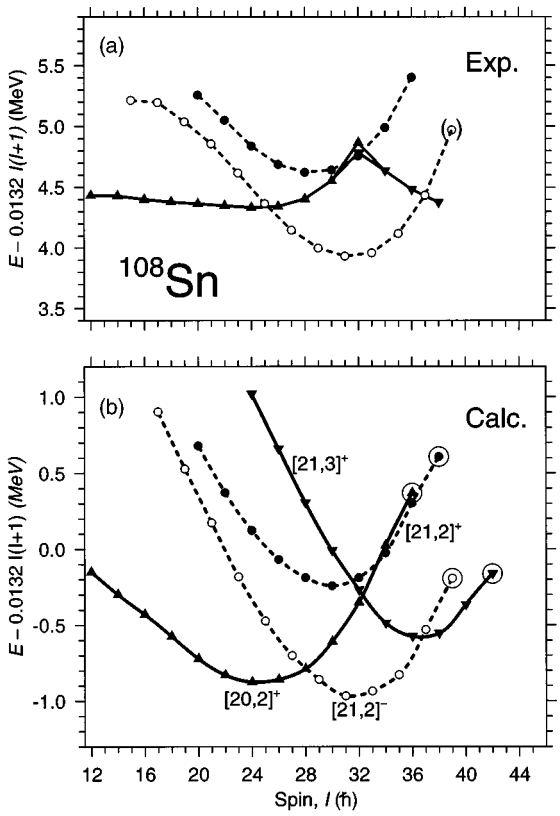


FIG. 4. Comparison between the lowest three calculated and experimentally observed rotational bands in $^{108}$Sn. In each case the same smooth rigid-rotor reference has been subtracted. The energy scales are different because the calculations are normalized to the liquid drop energy at spin zero, whilst in the experimental case the normalization is to the measured mass. Dashed (solid) lines indicate negative (positive) parity states. The terminating states for each of the configurations shown are indicated by large circles. The theoretical configurations shown are the lowest in the spin range of interest and are based on 2p-2h proton structures. Below spin $20\hbar$ other configurations based on 0p-0h and 1p-1h proton configurations are yrast. The nomenclature used in the theoretical calculations is $[p_1\ p_2,n]$ where $p_1$ is the number of proton holes in the $g_{9/2}$ orbital, $p_2$ is the number of $h_{11/2}$ protons and $n$ is the number of $h_{11/2}$ neutrons involved in the configuration.

Based on the comparison of the experimental moments of inertia between bands 2 and 3, the relative intensities of the two bands, the position where band 3 is observed to feed out to band 1, and the calculations shown in Fig. 4, we tenta-

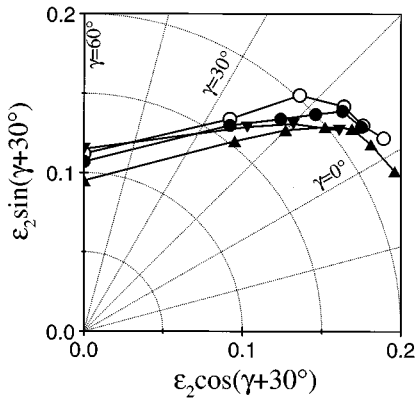


FIG. 5. $\epsilon$-$\gamma$ plot showing how the calculated nuclear shape evolves for the three structures discussed in the text. The terminating states are clearly seen to have $\gamma=60°$, whilst at low spin each of the bands is close to a prolate shape; i.e., $\gamma=0°$. Each data point shown is separated by $4\hbar$. The configurations shown are △ $\pi[g_{9/2}^{-2}\otimes(g_{7/2}d_{5/2})^2]\otimes\nu[(d_{5/2}g_{7/2})^6h_{11/2}^2]$ which terminates at spin $36^+$; ○ and ●, the favored and unfavored signatures of the $\pi[g_{9/2}^{-2}\otimes g_{7/2}^1h_{11/2}^1]\otimes\nu[(d_{5/2}g_{7/2})^6h_{11/2}^2]$ configuration which terminate at $39^-$ and $38^-$, respectively, and ▼ $\pi[g_{9/2}^{-2}\otimes g_{7/2}^1h_{11/2}^1]\otimes\nu[(d_{5/2}g_{7/2})^5h_{11/2}^3]$ which terminates at $42^+$. This latter configuration crosses the first one at spin $32\hbar$.

tively suggest that the remaining structure (band 3) can be associated with the unfavored signature of the $\pi[g_{9/2}^{-2}\otimes(g_{7/2}^1h_{11/2}^1)]\otimes\nu$ $[(d_{5/2}g_{7/2})^6h_{11/2}^2]$ configuration. If this assignment is correct then band 3 is also observed to the penultimate state before termination.

Figure 5 shows how the intrinsic nuclear shapes of the configurations discussed are predicted to change as a function of spin. According to calculations, at the bottom of the bands the nucleus is close to prolate ($\gamma\sim0°, \epsilon_2\sim0.2$) and so there is a collective rotation about an axis perpendicular to the symmetry axis. As the frequency increases, the spin vectors of the valence particles gradually align with this axis and this results in the nuclear shape slowly changing towards the noncollective single-particle shape ($\gamma\sim60°$). This gradual shape change within a single configuration has been termed ''soft'' or ''smooth'' band termination [4].

### C. Smooth termination in the $A\sim110$ mass region

Smoothly terminating bands have now been observed in several nuclei in the $A\sim110$ mass region. As discussed previously such structures, based on related 3p-2h proton configurations, are well known in Sb nuclei (e.g., [2,3,13,18, 19). It is interesting to note, however, that in $^{109}$Sb the three observed bands are all predicted to have the same 3p-2h proton configuration [i.e., $\pi(g_{9/2}^{-2}\otimes(g_{7/2}d_{5/2})^2)\otimes h_{11/2}$ [2, 14]. Here the three different structures are related to the different occupancy of the $g_{7/2}$, $d_{5/2}$ and $h_{11/2}$ neutron orbitals. Very recently a band with smooth termination properties has been reported in an odd mass tin isotope, $^{111}$Sn [20]. In this case, the 2p-2h proton structure is coupled to an $h_{11/2}$ neutron. Related structures have also been observed in Te nuclei (e.g., [14,21]), where the associated configurations are predicted to involve $\pi g[_{9/2}^{-2}\otimes(g_{7/2}d_{5/2})^2]\otimes h_{11/2}^2$ 4p-2h proton states. Evidence has also been established for the presence of smooth band termination behavior in the light iodine isotopes $^{113,115}$I, where 5p-2h proton structures are involved [22,23]. However, in the slightly heavier nucleus $^{117}$I smooth termination is not observed. Instead, abrupt termination (i.e., similar to that observed in $^{122}$Xe [6]) is seen in the yrast band, which is then followed by single-particle oblate yrast states [24]. This suggests that there may be a boundary between the two types of terminating bands.

In many of the smooth termination cases discussed above it has proved difficult to observe the structures close to termination as the nuclei concerned generally have several more protons and/or neutrons involved in the configurations than those in $^{108}$Sn and $^{109}$Sb, and hence the terminating spins are somewhat higher. In one particularly favorable case, however, in $^{114}$Te [14], a smoothly terminating band has been observed to spin $50\hbar$, which is close to termination.

## V. CONCLUSIONS

In conclusion, three rotational bands have been observed in $^{108}$Sn, and their structure can be successfully interpreted in terms of smoothly terminating bands based on 2p-2h proton structures. The configurations of the positive parity band and one of the negative parity bands have been established, and that of a third band tentatively assigned to be the signature partner of the negative parity band.

## ACKNOWLEDGMENTS

This work was supported by the U.S. National Science Foundation, AECL and by grants from the UK EPSRC, the Natural Sciences and Engineering Research Council of Canada and the Swedish Natural Science Research Council. K. H. acknowledges support from the University of York. We also wish to thank the crews of the Lawrence Berkeley 88″ cyclotron and the Chalk River TASCC laboratory tandem for providing the beams and to I.-Y. Lee and A. Macchiavelli for help with setting up Gammasphere.

[1] R. Wadsworth, H.R. Andrews, R.M. Clark, D.B. Fossan, A. Galindo-Uribarri, J.R. Hughes, V.P. Janzen, D.R. LaFosse, S.M. Mullins, E.S. Paul, D.C. Radford, H. Schnare, P. Vaska, D. Ward, J.N. Wilson, and R. Wyss, Nucl. Phys. **A559**, 461 (1993).

[2] V.P. Janzen, D.R. LaFosse, H. Schnare, D.B. Fossan, A. Galindo-Uribarri, J.R. Hughes, S.M. Mullins, E.S. Paul, L. Persson, S. Pilotte, D.C. Radford, I. Ragnarsson, P. Vaska, J.C. Waddington, R. Wadsworth, D. Ward, J. Wilson, and R. Wyss, Phys. Rev. Lett. **72**, 1160 (1994).

[3] D.R. LaFosse, D.B. Fossan, J.R. Hughes, Y. Liang, P. Vaska, M.P. Waring, and J.-y. Zhang, Phys. Rev. Lett. **69**, 1332 (1992).
[4] I. Ragnarsson, V.P. Janzen, D.B. Fossan, N.C. Schmeing, and R. Wadsworth, Phys. Rev. Lett. **74**, 3935 (1995).
[5] J. Simpson, M.A. Riley, S.J. Gale, J.F. Sharpey-Schafer, M.A. Bentley, A.M. Bruce, R. Chaapman, R.M. Clarke, S. Clarke, J. Copnell, D.M. Cullen, P. Fallon, A. Fitzpatrick, P.D. Forsyth, S.J. Freeman, P.M. Jones, M.J. Joyce, F. Liden, J.C. Lisle, A.O. Macchiavelli, A.G. Smith, J.F. Smith, J. Sweeney, D.M. Thompson, S. Warburton, J.N. Wilson, T. Bengtsson, and I. Ragnarsson, Phys. Lett. B **327**, 187 (1994), and references therein.
[6] J. Simpson, H. Timmers, M.A. Riley, T. Bengtsson, M.A. Bentley, F. Hanna, S.M. Mullins, J.F. Sharpey-Schafer, and R. Wyss, Phys. Lett. B **262**, 388 (1991).
[7] J. Bron, W.H.A. Hesselink, A. Van Poelgeest, J.J.A. Zalmstra, M.J. Uitzinger, and H. Verheul, Nucl. Phys. **A318**, 335 (1979).
[8] F. Azaiez, S. Andriamonje, J.F. Chemin, M. Fidah, J.N. Scheurer, M.M. Aleonard, G. Bastin, J.P. Thibaud, F. Beck, G. Costa, J.F. Bruandet, and F. Liatard, Nucl. Phys. **A501**, 401 (1989).
[9] D. Radford, Nucl. Instrum. Methods A **361**, 297 (1995).
[10] K.S. Krane, R.M. Steffen, and R.M. Wheeler, Nucl. Data Tables A **11**, 351 (1973).
[11] D. Ward, V.P. Janzen, H.R. Andrew, D.C. Radford, G.C. Ball, D. Horn, J.C. Waddington, J.K. Johansson, F. Banville, J. Gascon, S. Monarco, N. Nadon, S. Pilotte, D. Prévost, P. Taras, and R. Wyss, Nucl. Phys **A529**, 315 (1991).
[12] A.V. Afanasjev and I. Ragnarsson, Nucl. Phys. **A591**, 387 (1995).
[13] H. Schnare, D.R. LaFosse, D.B. Fossan, J.R. Hughes, P. Vaska, K. Hauschild, I.M. Hibbert, R. Wadsworth, V.P. Janzen, D.C. Radford, S.M. Mullins, C.W. Beausang, E.S. Paul, J. DeGraaf, and I. Ragnarsson, submitted to Phys. Rev. C.
[14] I. Thorslund, D.B. Fossan, D.R. LaFosse, H. Schnare, K. Hauschild, I.M. Hibbert, S.M. Mullins, E.S. Paul, I. Ragnarsson, J.M. Sears, P. Vaska, and R. Wadsworth, submitted to Phys. Rev. C **52**, R2839 (1995).
[15] R. Wadsworth, H.R. Andrews, C.W. Beausang, R.M. Clark, J. DeGraaf, D.B. Fossan, A. Galindo-Uribarri, I.M. Hibbert, K. Hauschild, J.R. Hughes, V.P. Janzen, D.R. LaFosse, S.M. Mullins, E.S. Paul, L. Persson, S. Pilotte, D.C. Radford, H. Schnare, P. Vaska, D. Ward, J.N. Wilson, and I. Ragnarsson, Phys. Rev. C **50**, 483 (1994).
[16] T. Bengtsson and I. Ragnarsson, Nucl. Phys. **A436**, 14 (1985).
[17] E.S. Paul *et al.*, Phys. Rev. C **50**, R534 (1994).
[18] V.P. Janzen, H.R. Andrews, B. Haas, D.C. Radford, D. Ward, A. Omar, D. Prévost, M. Sawicki, P. Unrau, J.C. Waddington, T.E. Drake, A. Galindo-Uribarri, and R. Wyss, Phys. Rev. Lett. **70**, 1065 (1993).
[19] D.R. LaFosse, D.B. Fossan, J.R. Hughes, Y. Liang, H. Schnare, P. Vaska, M.P. Waring, J-y. Zhang, R.M. Clark, R. Wadsworth, S.A. Forbes, E.S. Paul, V.P. Janzen, A. Galindo-Uribarri, D.C. Radford, D. Ward, S.M. Mullins, D. Prevost, and G. Zwartz, Phys. Rev. C **50**, 1819 (1994).
[20] D.R. Lafosse, D.B. Fossan, J.R. Hughes, Y. Liang, P. Vaska, M.P. Waring, J-y. Zhang, R.M. Clark, R. Wadsworth, S.A. Forbes, and E.S. Paul, Phys. Rev. C **51**, R2876 (1995).
[21] E.S. Paul, C.W. Beausang, S.A. Forbes, S.J. Gale, A.N. James, P.M. Jones, M.J. Joyce, H.R. Andrews, V.P. Janzen, D.C. Radford, D. Ward, R.M. Clark, K. Hauschild, I.M. Hibbert, R. Wadsworth, R.A. Cunningham, J. Simpson, T. Davinson, R.D. Page, P.J. Sellin, P.J. Woods, D.B. Fossan, D.R. LaFosse, H. Schnare, M.P. Waring, A. Gizon, J, Gizon, T.E. Drake, J. DeGraaf, and S. Pilotte, Phys. Rev. **C 50**, 698 (1994).
[22] M.P. Waring, E.S. Paul, C.W. Beausang, R.M. Clark, R.A. Cunningham, T. Davinson, S.A. Forbes, D.B. Fossan, S.J. Gale, A. Gizon, J. Gizon, K. Hauschild, I.M. Hibbert, A.N. James, P.M. Jones, M.J. Joyce, D.R. LaFosse, R.D. Page, I. Ragnarsson, H. Schnare, P.J. Sellin, J. Simpson, P. Vaska, R. Wadsworth, and P.J. Woods, Phys. Rev. C **51** 2427 (1995).
[23] E.S. Paul, H.R. Andrews, V.P. Janzen, D.C. Radford, D. Ward, T.E. Drake, J. DeGraaf, S. Pilotte, and I. Ragnarsson, Phys. Rev. C **50**, 741 (1994).
[24] E.S. Paul, D.B. Fossan, K. Hauschild, I.M. Hibbert, H. Schnare, J.M. Sears, I. Thorslund, R. Wadsworth, A.N. Wilson, and J.N. Wilson, Phys. Rev. C **51**, R2857 (1995).